Distributional Properties of Age of Information in Energy Harvesting Status Update Systems

Mohamed A. Abd-Elmagid and Harpreet S. Dhillon

***Abstract*—This paper considers an energy harvesting (EH) real-time status update system in which an EH-powered transmitter node sends *status updates* about some physical process of interest to a destination node. The status update and harvested energy packets are assumed to arrive at the transmitter according to independent Poisson processes, and the service time of each status update is assumed to be exponentially distributed. We quantify the freshness of status updates when they reach the destination using the concept of *Age of Information (AoI)*. Unlike most of the existing analyses of AoI that focus on characterizing its average when the transmitter has a reliable energy source and is hence not powered by EH (referred henceforth as a *non-EH transmitter*), our analysis is focused on understanding the *distributional properties* of AoI through the characterization of its moment generating function (MGF). In particular, we use the stochastic hybrid systems (SHS) framework to derive closed-form expressions of the MGF of AoI under both non-preemptive and preemptive in service queueing disciplines at the transmitter. We demonstrate the generality of this analysis by recovering several known results for the corresponding system with a non-EH transmitter as special cases of the new results. Our numerical results verify the analytical findings, and demonstrate the importance of incorporating the higher moments of AoI in the implementation/optimization of real-time status update systems rather than just relying on its average value.**

***Index Terms*—Age of information, energy harvesting, queueing systems, communication networks, stochastic hybrid systems.**

I. Introduction

The concept of AoI provides a rigorous way of quantifying the freshness of information in real-time status update systems, where a *transmitter node* aims to deliver timely status updates about some physical process of interest to a *destination node* [1]. For a queuing-theoretic model in which randomly generated status updates arrive at the transmitter according to a Poisson process, AoI was defined in [2] as the time elapsed since the latest successfully received status update at the destination was generated at the transmitter. The authors of [2] first derived a closed-form expression of the average AoI under first-come-first-served queueing discipline. The average value of AoI or peak AoI (an AoI-related metric which captures the peak values of AoI over time) was then characterized under several queueing disciplines in a series of subsequent works [3]–[6]. Further, a handful of recent works aimed to characterize the distribution (or some distributional properties) of AoI/peak AoI in the case of having a non-EH transmitter [7]–[10].

Due to the common ergodicity assumption of the AoI process in the above works, their analyses were mainly based on identifying the properties of the AoI sample functions and applying geometric arguments. These approaches require a careful choice of random variables for representing the AoI sample function, and often involve convoluted calculations of joint moments. This has motivated the authors of [11], [12] to build on the SHS framework of [13], and derive promising results allowing the use of the SHS approach for the queueuing-theoretic analyses of AoI. Following [11], [12], the SHS approach has been used to evaluate the average AoI in [14]–[17] and the MGF of AoI in [18] for a variety of queueing disciplines. Compared to the analyses of [14]–[18] considering a non-EH transmitter, the analysis of AoI using the SHS approach becomes much more challenging when the transmitter is powered by EH. This is due to the fact that the joint evolution of the battery state and the system occupancy with respect to the status updates has to be incorporated in the process of decision-making (i.e., the decisions of discarding or serving the new arriving status updates at the transmitter).

There have been a handful of prior works [19]–[22] analyzing AoI (by applying geometric arguments [19], [20] or by using the SHS approach [21], [22]) in the case where the transmitter node is powered by EH. However, the analyses of [19]–[22] have been limited to the evaluation of the average AoI. Different from these, this paper makes the first attempt to derive distributional properties of AoI through the characterization of its MGF. Before going into more details about our contributions, it is instructive to note that besides the above queueing theory-based analyses of AoI, there have also been efforts to optimize AoI or some other AoI-related metrics in different EH-powered communication systems that deal with time-sensitive information [23]–[27].

Contributions. This paper presents a novel queueing-theoretic analysis to characterize distributional properties of AoI at the destination in an EH status update system consisting of an EH-powered transmitter node, which is equipped with a battery of finite capacity. In particular, we use the SHS framework to derive closed-form expressions of the MGF of AoI at the destination under both non-preemptive and preemptive in service queueing disciplines at the transmitter. Since we consider an EH-powered transmitter here, the system discrete state is modeled as a two-dimensional continuous-time Markov chain to track both the numbers of update and harvested energy packets in the system. Using the MGF results, we further obtain closed-form expressions for both the first and second moments of AoI. We demonstrate that as the harvested energy arrival rate at the transmitter becomes large, the first and second moments of AoI for each queueing discipline converge to their counterparts in the case of having a non-EH transmitter. Our numerical results verify our analytical findings and reveal the impact of system design parameters on the achievable AoI performance by each queueing discipline.

The authors are with Wireless@VT, Department of ECE, Virginia Tech, Blacksburg, VA. Email: {maelaziz, hdhillon}@vt.edu. The support of the U.S. NSF (Grant CPS-1739642) is gratefully acknowledged.

ISBN 978-3-903176-37-9

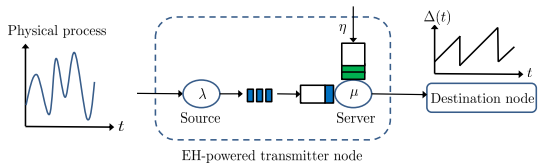

Fig. 1. An illustration of the system setup.

II. System Model

A. Network Model

We consider a real-time status update system in which an EH-powered transmitter node monitors some physical process, and sends its measurements to a destination node in the form of status update packets. As shown in Fig. 1, the transmitter node contains a single source generating the status update packets and a single server delivering the generated packets to the destination. Each status update packet carries some information about the value of the physical process and a time stamp indicating the time at which that information was measured. This system setup can be mapped to many scenarios of practical interest, such as an IoT network in which an aggregator (represents the transmitter node in our model) delivers sensed measurements to a destination node.

The status update packets are assumed to be generated by the source at the transmitter node according to a Poisson process with rate λ. Further, the transmitter harvests energy in the form of energy packets such that each energy packet contains the energy required for sending one status update packet to the destination node [19]–[22]. In particular, the harvested energy packets are assumed to arrive at the transmitter according to a Poisson process with rate η, and are stored in a battery queue of length B packets at the server (for serving the generated update packets). Given that the transmitter node has at least one energy packet in its battery queue, the time needed by its server to send a status update packet is assumed to be distributed as an exponential random variable with rate μ [2], [3], [5]. Let $\rho = \frac{\lambda}{\mu}$ and $\beta = \frac{\eta}{\mu}$ denote the server utilization and energy utilization factors, respectively.

We quantify the freshness of information status about the physical process at the destination (as a consequence of receiving update packets from the transmitter) using the concept of AoI. The formal definition of AoI is given below [2].

Definition 1. *Let t_i and t'_i denote the arrival and reception time instants of the i-th update packet at the transmitter and destination, respectively. Further, define $L(t)$ to be the index of the latest update packet received at the destination by time t, i.e., $L(t) = \max\{i|t'_i \leq t, \forall i\}$. Then, AoI is defined as the following random process*

$$\Delta(t) = t - t_{L(t)}. \tag{1}$$

B. Queueing Disciplines Considered in this Paper

For the above system setup, we analyze the AoI performance at the destination under two different queueing disciplines for managing update packet arrivals at the transmitter. In the following, we describe each of these queueing disciplines:

Last-come-first-served without preemption (LCFS-WP) queueing discipline. Under this queueing discipline, a new arriving update packet enters the service upon its arrival if the server is idle (i.e., the system is empty) and the battery contains at least one energy packet; otherwise, the new arriving update packet is discarded.

Last-come-first-served with preemption in service (LCFS-PS) queueing discipline. When the server is idle, the new arriving update packet under this queueing discipline is handled in the same way as in the LCFS-WP. However, when the server is busy, a new arriving packet replaces the current packet being served and the old packet in service is discarded.

As already conveyed, we consider that an energy packet contains the amount of energy required for transmitting one status update packet to the destination node. Therefore, we assume that the length of the energy battery queue reduces by one whenever a status update packet is successfully transmitted to the destination node. Further, with regards to the EH process, we consider that the transmitter node can harvest energy only if its server is idle[1] (i.e., there are no status update packets in the system). This case corresponds to the scenario where the transmitter is equipped with a single radio frequency (RF) chain and a single antenna, and thus can either transmit a status update packet or harvest energy at a certain time instant.

III. Problem Statement and Solution Approach

A. Problem Statement

Our goal is to analytically characterize the AoI performance at the destination node as a function of: i) the rate of status update packet arrivals λ, ii) the rate of harvesting energy packets η, iii) the rate of serving status update packets μ, and iv) the finite capacity of the energy battery queue B, at the transmitter node. Unlike most of the analyses of AoI in the literature, which were focused on deriving the average value of AoI, our analysis is focused on deriving distributional properties of AoI through the characterization of the MGF. A key benefit of this analysis lies in the fact that it allows one to judge the accuracy/reliability of solely relying on the average value of AoI in the design/optimization of real-time status update systems. As will be demonstrated in Section V, the implementation of real-time status update systems based on just the average value of AoI does not ensure reliability, and it is crucial to incorporate the higher moments of AoI in the design of such systems. This, in turn, highlights the significance of the analytical distributional properties of AoI derived in this paper.

B. Stochastic Hybrid Systems: A Brief Introduction

To derive the MGF of AoI for the considered queueing disciplines at the transmitter node (presented in Subsection II-B), we resort to the SHS framework in [13], which was first tailored for the analysis of AoI in [11] and [12]. In the following, we provide a very brief[2] description of the SHS framework, which will be useful in understanding our AoI

[1]Our analysis is extended to the case where the transmitter can harvest energy anytime (i.e., even its server is busy) in the expanded journal submission of this paper [28].

[2]Interested readers are advised to refer to [11] and [12] for a detailed discussion about the use of the SHS approach in the analysis of AoI.

ISBN 978-3-903176-37-9 © 2021 IFIP

MGF analysis in the next section. The SHS technique is used to analyze hybrid queueing systems that can be modeled by a combination of discrete and continuous state parameters. In particular, the SHS technique models the discrete state of the system $q(t) \in \mathcal{Q} = \{1, \cdots, m\}$ by a continuous-time finite-state Markov chain, where $\mathcal{Q}$ is the discrete state space. This continuous-time Markov chain governs the dynamics of the system discrete state that usually describes the system occupancy, e.g., $q(t)$ represents the numbers of status update and energy packets in the system for our problem. On the other hand, the evolution of the system continuous state is described by a continuous process $\mathbf{x}(t) = [x_0(t), \cdots, x_n(t)] \in \mathbb{R}^{1\times(n+1)}$, e.g., $x(t)$ models the evolution of the age-related processes in our system setting.

A transition $l \in \mathcal{L}$ from state q_l to state q'_l (in the Markov chain modeling $q(t)$) occurs due to the arrival of a status update/energy packet or the delivery of a status update to the destination (i.e., the departure of a status update from the system), where $\mathcal{L}$ denotes the set of all transitions. Therefore, the transition l takes place with the exponential rate $\lambda^{(l)}\delta_{q_l,q(t)}$ due to the fact that the time elapsed between departures and arrivals is exponentially distributed, where the Kronecker delta function $\delta_{q_l,q(t)}$ ensures that the transition l occurs only when the discrete state $q(t)$ is equal to q_l. As a consequence of the occurrence of transition l, the discrete state of the system changes from state q_l to state q'_l, and the continuous state $\mathbf{x}$ is reset to $\mathbf{x}'$ according to a binary reset map matrix $\mathbf{A}_l \in \mathbb{B}^{(n+1)\times(n+1)}$ as $\mathbf{x}' = \mathbf{x}\mathbf{A}_l$. Further, $\dot{\mathbf{x}}(t) \triangleq \dfrac{\partial \mathbf{x}(t)}{\partial t} = \mathbf{1}$ holds as long as the state $q(t)$ is unchanged, where $\mathbf{1}$ is the row vector $[1, \cdots, 1] \in \mathbb{R}^{1\times(n+1)}$. Different from ordinary continuous-time Markov chains, an inherent feature of SHSs is the possibility of having self-transitions in the Markov chain modeling the system discrete state. In particular, although a self-transition keeps $q(t)$ unchanged, it causes a change in the continuous process $x(t)$.

Now, we define some useful quantities for the characterization of the MGF of AoI at the destination node using the SHS technique. Denote by $\pi_q(t)$ the probability of being in state q of the continuous-time Markov chain at time t. Further, let $\mathbf{v}_q(t) = [v_{q0}(t), \cdots, v_{qn}(t)] \in \mathbb{R}^{1\times(n+1)}$ denote the correlation vector between $q(t)$ and $x(t)$, and $\mathbf{v}^s_q(t) = [v^s_{q0}(t), \cdots, v^s_{qn}(t)] \in \mathbb{R}^{1\times(n+1)}$ denote the correlation vector between $q(t)$ and the exponential function $e^{s\mathbf{x}(t)}$, where $s \in \mathbb{R}$. Thus, we can respectively express $\pi_q(t)$, $\mathbf{v}_q(t)$ and $\mathbf{v}^s_q(t)$ as

$$\pi_q(t) = \Pr\left(q(t) = q\right) = \mathbb{E}[\delta_{q,q(t)}],\ \forall q \in \mathcal{Q}, \tag{2}$$

$$\mathbf{v}_q(t) = [v_{q0}(t), \cdots, v_{qn}(t)] = \mathbb{E}[\mathbf{x}(t)\delta_{q,q(t)}],\ \forall q \in \mathcal{Q}, \tag{3}$$

$$\mathbf{v}^s_q(t) = [v^s_{q0}(t), \cdots, v^s_{qn}(t)] = \mathbb{E}[e^{s\mathbf{x}(t)}\delta_{q,q(t)}],\ \forall q \in \mathcal{Q}. \tag{4}$$

According to the ergodicity assumption of the continuous-time Markov chain modeling $q(t)$ in the AoI analysis [11], [12], the state probability vector $\pi(t) = [\pi_0(t), \cdots, \pi_m(t)]$ converges uniquely to the stationary vector $\bar{\pi} = [\bar{\pi}_0, \cdots, \bar{\pi}_m]$ satisfying

$$\bar{\pi}_q \sum_{l\in\mathcal{L}_q} \lambda^{(l)} = \sum_{l\in\mathcal{L}'_q} \lambda^{(l)}\bar{\pi}_{q_l},\ q \in \mathcal{Q},\ \sum_{q\in\mathcal{Q}} \bar{\pi}_q = 1, \tag{5}$$

where $\mathcal{L}'_q = \{l \in \mathcal{L} : q'_l = q\}$ and $\mathcal{L}_q = \{l \in \mathcal{L} : q_l = q\}$ denote the sets of incoming and outgoing transitions for state $q, \forall q \in \mathcal{Q}$.

Using the above notations, it has been shown in [12, Theorem 1] that under the ergodicity assumption of the Markov chain modeling $q(t)$, if we can find a non-negative limit $\bar{\mathbf{v}}_q = [\bar{v}_{q0}, \cdots, \bar{v}_{qn}],\ \forall q \in \mathcal{Q}$, for the correlation vector $\mathbf{v}_q(t)$ satisfying

$$\bar{\mathbf{v}}_q \sum_{l\in\mathcal{L}_q} \lambda^{(l)} = \bar{\pi}_q\mathbf{1} + \sum_{l\in\mathcal{L}'_q} \lambda^{(l)}\bar{\mathbf{v}}_{q_l}\mathbf{A}_l,\ q \in \mathcal{Q}, \tag{6}$$

then:

- The expectation of $x(t)$, $\mathbb{E}[x(t)]$, converges to the following stationary vector:
$$\mathbb{E}[x] = \sum_{q\in\mathcal{Q}} \bar{\mathbf{v}}_q. \tag{7}$$
- There exists $s_0 > 0$ such that for all $s < s_0$, $\mathbf{v}^s_q(t)$ converges to $\bar{\mathbf{v}}^s_q$ that satisfies
$$\bar{\mathbf{v}}^s_q \sum_{l\in\mathcal{L}_q} \lambda^{(l)} = s\bar{\mathbf{v}}^s_q + \sum_{l\in\mathcal{L}'_q} \lambda^{(l)}[\bar{\mathbf{v}}^s_{q_l}\mathbf{A}_l + \bar{\pi}_{q_l}\mathbf{1}\hat{\mathbf{A}}_l],\ q \in \mathcal{Q}, \tag{8}$$
where $\hat{\mathbf{A}}_l \in \mathbb{B}^{(n+1)\times(n+1)}$ is a binary matrix whose elements are constructed as: $\hat{\mathbf{A}}_l(k,j) = 1$ if $k = j$ and the j-th column of $\mathbf{A}_l$ is a zero vector; otherwise, $\hat{\mathbf{A}}_l(k,j) = 0$. Further, the MGF of the state $\mathbf{x}(t)$, which can be obtained as $\mathbb{E}[e^{s\mathbf{x}(t)}]$, converges to the following stationary vector:
$$\mathbb{E}[e^{s\mathbf{x}}] = \sum_{q\in\mathcal{Q}} \bar{\mathbf{v}}^s_q. \tag{9}$$

From (7) and (9), when the first element of the continuous state $\mathbf{x}(t)$ represents the AoI at the destination node, the expectation and the MGF of AoI at the destination node respectively converge to:

$$\overset{(1)}{\Delta} = \sum_{q\in\mathcal{Q}} \bar{v}_{q0}, \tag{10}$$

$$M(s) = \sum_{q\in\mathcal{Q}} \bar{v}^s_{q0}. \tag{11}$$

IV. The MGF Analysis of the Queueing Disciplines Considered in this Paper

In this section, we present the analysis of the MGF of AoI for the two queueing disciplines considered in this paper. Using the notations of the SHS approach (presented in Subsection III-B), the discrete state space $\mathcal{Q}$ in each queueing discipline is given by $\mathcal{Q} = \{1, 2, \cdots, 2B+1\}$. As shown in Fig. 2, each state in $\mathcal{Q}$ represents a potential combination of the number of update packets in the system and the number of energy packets in the battery queue at the server. For instance, a state $j = (e_j, u_j)$ indicates that the system has u_j status update packets and the energy battery queue at the server contains e_j energy packets. Note that since the system can have at most one status update packet at any time instant in both queueing disciplines, we have $u_j \in \{0, 1\}$. In particular, $u_j = 0$ indicates that the system is empty and hence the server is idle, and $u_j = 1$ indicates that the server

ISBN 978-3-903176-37-9 © 2021 IFIP

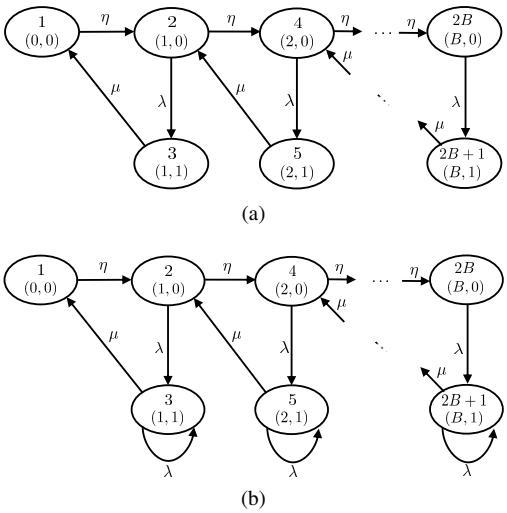

Fig. 2. Markov chains modeling the discrete state of the system: (a) LCFS-WP queueing discipline, and (b) LCFS-PS queueing discipline.

is serving the existing update packet in the system. Further, since the battery queue at the server has a capacity of B packets, we have $e_j \in \{0, 1, \cdots, B\}$. On the other hand, the continuous process $\mathbf{x}(t)$ in each queueing discipline is given by $\mathbf{x}(t) = [x_0(t), x_1(t)]$, where $x_0(t)$ represents the value of AoI at the destination node at time instant t, and $x_1(t)$ indicates the value that the AoI at the destination node will become if the existing update packet in the system completes its service at time instant t (i.e., the packet is delivered to the destination at t). Recall from Subsection III-B that as long as there is no change (due to the arrival/departure of an update/energy packet) in the discrete state $q(t)$, we have $\frac{\partial \mathbf{x}(t)}{\partial t} = 1$, i.e., the elements of the age vector $\mathbf{x}(t)$ increase linearly with time.

A. LCFS-WP Queueing Discipline

The continuous-time Markov chain modeling the discrete state of the system $q(t)$ is depicted in Fig. 2a. We denote the set of states in the $i-$th row of the Markov chain by r_i. Further, Table I presents the set of different transitions $\mathcal{L}$ and their impact on the values of both $q(t)$ and $\mathbf{x}(t)$. Before proceeding into evaluating the MGF of AoI at the destination using (5)-(11), we first describe the set of transitions as follows:

$l = 3k-2$: This subset of transitions takes place between the states of the Markov chain in r_1, corresponding to the time when the system is empty. In particular, a transition from this set of transitions occurs when a new energy packet is harvested by the transmitter. Clearly, since harvesting a new energy packet does not impact the value of AoI at the destination node, we observe that the first element in the updated value of the age vector $\mathbf{x}\mathbf{A}_l$ (as a consequence of this transition) is x_0, i.e., this transition does not induce any change in the value of AoI at the destination. Further, since the server is idle in the states of r_1, the second component of $\mathbf{x}(t)$ (quantifying the age of the packet in service) becomes irrelevant for such set of states. Note that whenever a component of $\mathbf{x}(t)$ is/becomes irrelevant after the occurrence of some transition l, its value in the updated age vector $\mathbf{x}\mathbf{A}_l$ can be set arbitrarily. Following the convention [11], we set the value corresponding to such irrelevant components in the updated age value to 0, and thus we observe that the second component of $\mathbf{x}\mathbf{A}_{3k-2}$ is 0.

$l = 3k-1$: A transition from this subset of transitions occurs when there is a new arriving update packet at the transmitter node. Since the age of this new arriving update packet at the transmitter is 0 and it does not have any impact on the AoI value at the destination, we note that the updated age vector $\mathbf{x}\mathbf{A}_l$ is set to be $[x_0, 0]$.

$l = 3k$: This subset of transitions occurs when an update packet is delivered to the destination. As a consequence of this transition, the AoI value at the destination is reset to the age of the new received update packet, and thus the first component of $\mathbf{x}\mathbf{A}_l$ is x_1. In addition, since the system becomes empty after the occurrence of this transition, the second component of the age vector $\mathbf{x}(t)$ becomes irrelevant, and thus its corresponding value in the updated age vector $\mathbf{x}\mathbf{A}_l$ is 0.

Now, recall that in order to use (8) to derive the MGF of AoI at the destination, one needs to find a non-negative limit $\bar{\mathbf{v}}_q, \forall q \in \mathcal{Q}$, satisfying (6). It can be shown that this condition holds for the two queueing disciplines studied in this paper by solving the set of equations in (6). In particular, the solution of the set of equations in (6) can be obtained along the same lines of the analysis presented in this paper for characterizing the MGF of AoI at the destination node. Thus, for the sake of brevity, we next focus on evaluating $\bar{v}^s_{q0}, \forall q \in \mathcal{Q}$, satisfying the set of equations in (8), using which the MGF of AoI at the destination can be calculated as in (11). By inspecting (8), we observe that the steady state probabilities $\bar{\pi}_q, q \in \mathcal{Q}$, and the two vectors $\bar{\mathbf{v}}^s_{q_l}\mathbf{A}_l$ and $\bar{\pi}_{q_l}\mathbf{1}\hat{\mathbf{A}}_l$ (associated with each transition l in $\mathcal{L}$) need to be computed. The calculations of $\bar{\mathbf{v}}^s_{q_l}\mathbf{A}_l$ and $\bar{\pi}_{q_l}\mathbf{1}\hat{\mathbf{A}}_l$, $l \in \mathcal{L}$, are listed in Table I, and the steady state probabilities $\bar{\pi}_q, q \in \mathcal{Q}$ are given by the following proposition.

Proposition 1. *The steady state probabilities $\{\bar{\pi}_i\}$ can be expressed as*

$$\bar{\pi}_{2i} = \left(\frac{\beta}{\rho}\right)^i \bar{\pi}_1, \tag{12}$$

$$\bar{\pi}_{2i+1} = \rho\left(\frac{\beta}{\rho}\right)^i \bar{\pi}_1, \tag{13}$$

where $1 \leq i \leq B$ and $\bar{\pi}_1$ is given by

$$\bar{\pi}_1 = \begin{cases} \dfrac{1}{1+B(1+\rho)}, & \text{if } \rho = \beta, \\ \dfrac{\rho^B(\beta-\rho)}{\rho^B(\beta-\rho)+\beta(1+\rho)(\beta^B-\rho^B)}, & \text{otherwise.} \end{cases} \tag{14}$$

Proof: See Appendix A. ∎

Having the steady state probabilities $\{\bar{\pi}_q\}$ in Proposition 1 and the set of transitions $\mathcal{L}$ in Table I, we are now ready to use (8) for deriving the MGF of AoI at the destination in the following theorem.

Theorem 1. *The MGF of AoI for the LCFS-WP queueing discipline is given by*

$$\overset{\text{WP}}{M}(\bar{s}) = \frac{\rho\bar{\pi}_1\left[\bar{s}^2\theta - \bar{s}\theta(1+\rho+\beta) + \beta(1+\theta+\theta\rho)\right]}{(1-\bar{s})^2(\rho-\bar{s})(\beta-\bar{s})}, \tag{15}$$

ISBN 978-3-903176-37-9 © 2021 IFIP

TABLE I
TRANSITIONS OF THE LCFS-WP QUEUEING DISCIPLINE IN FIG. 2A ($2 \leq k \leq B$).

l	$q_l \to q_l'$	$\lambda^{(l)}$	$\mathbf{x}\mathbf{A}_l$	$\mathbf{A}_l$	$\hat{\mathbf{A}}_l$	$\bar{\mathbf{v}}_{q_l}^s \mathbf{A}_l$	$\bar{\pi}_{q_l} \mathbf{1} \hat{\mathbf{A}}_l$
1	$1 \to 2$	η	$[x_0, 0]$	$\begin{bmatrix} 1 & 0 \\ 0 & 0 \end{bmatrix}$	$\begin{bmatrix} 0 & 0 \\ 0 & 1 \end{bmatrix}$	$[\bar{v}_{10}^s, 0]$	$[0, \bar{\pi}_1]$
2	$2 \to 3$	λ	$[x_0, 0]$	$\begin{bmatrix} 1 & 0 \\ 0 & 0 \end{bmatrix}$	$\begin{bmatrix} 0 & 0 \\ 0 & 1 \end{bmatrix}$	$[\bar{v}_{20}^s, 0]$	$[0, \bar{\pi}_2]$
3	$3 \to 1$	μ	$[x_1, 0]$	$\begin{bmatrix} 0 & 0 \\ 1 & 0 \end{bmatrix}$	$\begin{bmatrix} 0 & 0 \\ 0 & 1 \end{bmatrix}$	$[\bar{v}_{31}^s, 0]$	$[0, \bar{\pi}_3]$
$3k-2$	$2k-2 \to 2k$	η	$[x_0, 0]$	$\begin{bmatrix} 1 & 0 \\ 0 & 0 \end{bmatrix}$	$\begin{bmatrix} 0 & 0 \\ 0 & 1 \end{bmatrix}$	$[\bar{v}_{2k-2,0}^s, 0]$	$[0, \bar{\pi}_{2k-2}]$
$3k-1$	$2k \to 2k+1$	λ	$[x_0, 0]$	$\begin{bmatrix} 1 & 0 \\ 0 & 0 \end{bmatrix}$	$\begin{bmatrix} 0 & 0 \\ 0 & 1 \end{bmatrix}$	$[\bar{v}_{2k,0}^s, 0]$	$[0, \bar{\pi}_{2k}]$
$3k$	$2k+1 \to 2k-2$	μ	$[x_1, 0]$	$\begin{bmatrix} 0 & 0 \\ 1 & 0 \end{bmatrix}$	$\begin{bmatrix} 0 & 0 \\ 0 & 1 \end{bmatrix}$	$[\bar{v}_{2k+1,1}^s, 0]$	$[0, \bar{\pi}_{2k+1}]$

TABLE II
TRANSITIONS OF THE LCFS-PS QUEUEING DISCIPLINE IN FIG. 2B ($2 \leq k \leq B$).

l	$q_l \to q_l'$	$\lambda^{(l)}$	$\mathbf{x}\mathbf{A}_l$	$\mathbf{A}_l$	$\hat{\mathbf{A}}_l$	$\bar{\mathbf{v}}_{q_l}^s \mathbf{A}_l$	$\bar{\pi}_{q_l} \mathbf{1} \hat{\mathbf{A}}_l$
$3B+k-1$	$2k-1 \to 2k-1$	λ	$[x_0, 0]$	$\begin{bmatrix} 1 & 0 \\ 0 & 0 \end{bmatrix}$	$\begin{bmatrix} 0 & 0 \\ 0 & 1 \end{bmatrix}$	$[\bar{v}_{2k-1,0}^s, 0]$	$[0, \bar{\pi}_{2k-1}]$

where $\bar{s} = \frac{s}{\mu}$ and θ can be expressed as

$$\theta = \begin{cases} B, & \text{if } \rho = \beta, \\ \dfrac{\beta\left(\beta^B - \rho^B\right)}{\rho^B\left(\beta - \rho\right)}, & \text{otherwise.} \end{cases} \tag{16}$$

Proof: See Appendix B. ∎

Corollary 1. *Using $\overset{\text{WP}}{M}(\bar{s})$ derived in Theorem 1, the first moment of AoI in the LCFS-WP queueing discipline can be expressed as*

$$\overset{(1)}{\Delta}_{\text{WP}} = \begin{cases} \dfrac{2B\rho^2 + 2\left(1+B\right)\rho + B + 2}{\mu\left[B\rho^2 + (1+B)\rho\right]}, & \text{if } \rho = \beta, \\ \dfrac{\beta^{B+2}\left(2\rho^2 + 2\rho + 1\right) - \rho^{B+2}\left(2\beta^2 + 2\beta + 1\right)}{\mu\left[\beta^{B+2}\left(\rho^2 + \rho\right) - \rho^{B+2}\left(\beta^2 + \beta\right)\right]}, \end{cases} \tag{17}$$

where the second case in (17) holds when $\rho \neq \beta$. Further, the second moment of AoI $\overset{(2)}{\Delta}_{\text{WP}}$ is given by (18) [at the top of the next page].

Proof: The expression of $\overset{\text{WP}}{M}(\bar{s})$ (derived in Theorem 1) can be used to compute the k-th moment of AoI (denoted by $\overset{(k)}{\Delta}_{\text{WP}}$) as follows

$$\overset{(k)}{\Delta}_{\text{WP}} = \frac{1}{\mu^k} \times \frac{\mathrm{d}^k\left[\overset{\text{WP}}{M}(\bar{s})\right]}{\mathrm{d}\bar{s}^k}\Big|_{\bar{s}=0}, \tag{19}$$

where $\frac{\mathrm{d}^k}{\mathrm{d}\bar{s}^k}$ denotes the k-th derivative with respect to $\bar{s}$. Evaluating this for $k \in \{1, 2\}$ completes the proof. ∎

Remark 1. *Note that the expression of $\overset{(1)}{\Delta}_{\text{WP}}$ in (17) is identical to the average AoI expression derived in [21, Theorem 3]. Further, when $\beta \to \infty$, $\overset{(1)}{\Delta}_{\text{WP}}$ and $\overset{(2)}{\Delta}_{\text{WP}}$ in the case of $\rho \neq \beta$ reduce to*

$$\lim_{\beta\to\infty} \overset{(1)}{\Delta}_{\text{WP}} = \frac{2\rho^2 + 2\rho + 1}{\mu\left(\rho^2 + \rho\right)},$$
$$\lim_{\beta\to\infty} \overset{(2)}{\Delta}_{\text{WP}} = \frac{2\left(3\rho^3 + 3\rho^2 + 2\rho + 1\right)}{\mu^2\rho^2\left(1+\rho\right)}. \tag{20}$$

Clearly, $\overset{(1)}{\Delta}_{\text{WP}}$ reduced to the average AoI expression derived in [5] for the M/M/1/1 case considering a non-EH transmitter, and $\overset{(2)}{\Delta}_{\text{WP}}$ reduced to the second moment of AoI for the same case.

Remark 2. *As was the case for $\overset{(1)}{\Delta}_{\text{WP}}$ (given by (17)) in [21], we observe from (18) that $\overset{(2)}{\Delta}_{\text{WP}}$ is invariant to exchanging ρ and β when $\rho \neq \beta$. Clearly, this is a counterintuitive insight since the energy and update packets are managed by the transmitter node in a totally different manner, i.e., the capacity of the battery queue at the server is B energy packets whereas under the LCFS-WP queueing discipline, there can be at most one update packet in the system (in service) at any time instant.*

B. LCFS-PS Queueing Discipline

Fig. 2b depicts the Markov chain representing discrete state of the system. The set of transitions in this queueing discipline can be constructed using Tables I and II. The subset of transitions $l = 3B + k - 1, 2 \leq k \leq B$, in Table II refers to the event of having a new arriving update packet at the transmitter node while its server is serving another update packet. According to the mechanism of the LCFS-PS queueing discipline, the status update that is currently being served will be discarded, and the new arriving one will enter the service upon its arrival. Since the new arriving update packet does not influence the AoI value at the destination and its age is 0, the updated age vector is given by $[x_0, 0]$. Furthermore, from (5), we note that the self-transitions do not impact the values of the steady state probabilities $\{\pi_i\}$, and hence $\{\pi_i\}$ in this case can be obtained using Proposition 1. That said, the MGF of AoI at the destination is provided in the next theorem.

Theorem 2. *The MGF of AoI for the LCFS-PS queueing discipline is given by*

$$\overset{\text{PS}}{M}(\bar{s}) = \frac{\rho\left(1+\rho\right)\bar{\pi}_1\Big[\bar{s}^2\theta - \bar{s}\theta\left(1+\rho+\beta\right) + \beta\left(1+\theta+\theta\rho\right)\Big]}{\left(1-\bar{s}\right)\left(\rho-\bar{s}\right)\left(1+\rho-\bar{s}\right)\left(\beta-\bar{s}\right)}. \tag{21}$$

Proof: See Appendix C. ∎

Corollary 2. *Using $\overset{\text{PS}}{M}(\bar{s})$ derived in Theorem 2, the first moment of AoI in the LCFS-PS queueing discipline can be expressed as*

$$\overset{(1)}{\Delta}_{\text{PS}} = \begin{cases} \dfrac{B\rho^3 + (3B+1)\rho^2 + (3B+4)\rho + B + 2}{\mu\rho\left(1+\rho\right)\left(\rho B + B + 1\right)}, & \text{if } \rho = \beta, \\ \dfrac{\beta^{B+2}\left(1+\rho\right)^3 - \rho^{B+2}\Big[\left(\beta^2+\beta\right)\left(\rho+2\right) + 1 + \rho\Big]}{\mu\left(1+\rho\right)\left[\beta^{B+2}\left(\rho^2+\rho\right) - \rho^{B+2}\left(\beta^2+\beta\right)\right]}, \end{cases} \tag{22}$$

where the second case in (22) holds when $\rho \neq \beta$. Further, the second moment of AoI $\overset{(2)}{\Delta}_{\text{PS}}$ is given by (23) [at the top of next page].

Remark 3. *When $\beta \to \infty$, $\overset{(1)}{\Delta}_{\text{PS}}$ and $\overset{(2)}{\Delta}_{\text{PS}}$ (in (22) and (23) for the case $\rho \neq \beta$) reduce to*

$$\lim_{\beta\to\infty} \overset{(1)}{\Delta}_{\text{PS}} = \frac{1}{\lambda} + \frac{1}{\mu}, \quad \lim_{\beta\to\infty} \overset{(2)}{\Delta}_{\text{PS}} = 2\Big[\frac{1}{\lambda^2} + \frac{1}{\mu\lambda} + \frac{1}{\mu^2}\Big], \tag{24}$$

ISBN 978-3-903176-37-9 © 2021 IFIP

$$\overset{(2)}{\Delta}_{\rm WP} = \begin{cases} \dfrac{2\left[3B\rho^3+(3B+3)\rho^2+(2B+4)\rho+B+3\right]}{\mu^2\rho^2(1+B+B\rho)}, & \text{if } \rho=\beta, \\ \dfrac{2\left[\beta^{B+3}\left(3\rho^3+3\rho^2+2\rho+1\right)-\rho^{B+3}\left(3\beta^3+3\beta^2+2\beta+1\right)\right]}{\mu^2\left[\beta^{B+3}\rho^2(1+\rho)-\rho^{B+3}\beta^2(\beta+1)\right]}, & \text{otherwise.} \end{cases} \tag{18}$$

$$\overset{(2)}{\Delta}_{\rm PS} = \begin{cases} \dfrac{2\left[B\rho^5+(4B+1)\rho^4+(7B+5)\rho^3+(7B+12)\rho^2+(4B+10)\rho+B+3\right]}{\mu^2\rho^2(1+\rho)^2(1+B+B\rho)}, & \text{if } \rho=\beta, \\ \dfrac{2\beta^{B+3}(1+\rho)^3\left(1+\rho+\rho^2\right)-2\rho^{B+3}\left[\left(\beta^3+\beta^2+\beta\right)\left(\rho^2+3\rho+2\right)+\beta^3+\beta^2+(1+\rho)^2\right]}{\mu^2(1+\rho)^2\left[\beta^{B+3}\rho^2(1+\rho)-\rho^{B+3}\beta^2(1+\beta)\right]}, & \text{otherwise.} \end{cases} \tag{23}$$

which match the first and second moments of AoI for the LCFC-PS queueing discipline in [11, Theorem 2(a)] considering a non-EH transmitter.

Remark 4. *Note that from Corollaries 1 and 2, we have*

$$\overset{(1)}{\Delta}_{\rm WP} - \overset{(1)}{\Delta}_{\rm PS} = \begin{cases} \dfrac{B\rho^2+\rho(B+1)+B}{\mu\left[B\rho^2+\rho(2B+1)+B+1\right]}, & \text{if } \rho=\beta, \\ \dfrac{\rho}{\mu(1+\rho)}, & \text{otherwise,} \end{cases} \tag{25}$$

and $\overset{(2)}{\Delta}_{\rm WP} - \overset{(2)}{\Delta}_{\rm PS}$ *is given by (26) [at the top of the next page]. We observe from (25) and (26) that* $\overset{(1)}{\Delta}_{\rm WP} - \overset{(1)}{\Delta}_{\rm PS} \geq 0$ *and* $\overset{(2)}{\Delta}_{\rm WP} - \overset{(2)}{\Delta}_{\rm PS} \geq 0$ *for any choice of values of the system parameters. This indicates the superiority of the LCFS-PS queueing discipline over the LCFS-WP one, in terms of the achievable AoI performance at the destination node. We further observe that when* $\rho \neq \beta$, $\overset{(1)}{\Delta}_{\rm WP} - \overset{(1)}{\Delta}_{\rm PS}$ *does not depend on the parameters related to the EH process (i.e.,* β *and* B*), and the difference monotonically increases as a function of* ρ *from* $\lim_{\rho\to 0} \overset{(1)}{\Delta}_{\rm WP} - \overset{(1)}{\Delta}_{\rm PS} = 0$ *until it approaches* $\lim_{\rho\to\infty} \overset{(1)}{\Delta}_{\rm WP} - \overset{(1)}{\Delta}_{\rm PS} = \frac{1}{\mu}$*. On the other hand,* $\overset{(2)}{\Delta}_{\rm WP} - \overset{(2)}{\Delta}_{\rm PS}$ *monotonically increases as a function of* ρ *from* $\lim_{\rho\to 0} \overset{(2)}{\Delta}_{\rm WP} - \overset{(2)}{\Delta}_{\rm PS} = \frac{2}{\mu^2}$ *until it approaches* $\lim_{\rho\to\infty} \overset{(2)}{\Delta}_{\rm WP} - \overset{(2)}{\Delta}_{\rm PS} = \dfrac{4\beta^2+4\beta+2}{\mu^2\beta(1+\beta)}$.

V. Numerical Results

Verification of analytical results. In Figs. 3a and 3b, we verify the accuracy of the analytical expressions of the first and second moments of AoI (obtained using the MGFs derived in Theorems 1 and 2) by comparing them to their simulated counterparts (obtained numerically using [12, Theorem 1]). We observe a perfect match between the analytical and simulated curves. As expected, we further observe that as β increases, the achievable AoI performance by each queueing discipline improves until it converges to its counterpart with a non-EH transmitter (represented by $\beta = 50$). In particular, Fig. 3a shows that $\overset{(1)}{\Delta}_{\rm WP}$ and $\overset{(2)}{\Delta}_{\rm WP}$ converge to their corresponding ones in the M/M/1/1 case of [5] (as stated in Remark 1), and Fig. 3b shows that $\overset{(1)}{\Delta}_{\rm PS}$ and $\overset{(2)}{\Delta}_{\rm PS}$ converge to their counterparts in the single-source case of [11, Theorem 2(a)] (as stated in Remark 3).

Impact of the battery capacity on the achievable AoI performance. In Figs. 3c and 3d, we show the impact of B on the achievable AoI performance for the considered queueing disciplines. Clearly, increasing B increases the likelihood that the battery queue will have sufficient energy required for serving update packets upon their arrivals (when the server is idle), and hence the achievable AoI performance by each queueing discipline improves with increasing B. It is also worth noting that as $B \to \infty$, the achievable AoI performance by each queueing discipline approaches the AoI performance of its counterpart with a non-EH transmitter. That said, there may still be a slight gap between the two due to the finite rate of harvesting energy.

Comparison between the LCFS-WP and LCFS-PS queueing disciplines. Figs. 3e and 3f compare the LCFS-WP and LCFS-PS queueing disciplines in terms of the achievable AoI performance. We observe the superiority of the LCFS-PS queueing discipline over the LCFS-WP one in terms of the achievable first and second moments of AoI at the destination, which supports our arguments in Remark 4. We further observe that the standard deviation of AoI σ associated with each queueing discipline is relatively large (with respect to the average value $\overset{(1)}{\Delta}$). This is indeed a key insight indicating the necessity of incorporating the higher moments of AoI in the implementation/optimization of real-time status update systems rather than just relying on the average value (as has been mostly done in the existing literature on AoI). This insight demonstrates the importance of the analytical expressions of the second moment of AoI derived in this paper for the considered queueing disciplines.

VI. Conclusion

This paper presented a queueing theory-based analysis of AoI to characterize its distributional properties in EH status update systems. In particular, the SHS approach was used to derive closed-form expressions of the MGF of AoI at the destination under both non-preemptive (LCFS-WP) and preemptive in service (LCFS-PS) queueing disciplines at the transmitter. Our analytical results allowed us to obtain several interesting (and some even counterintuitive) insights regarding the

ISBN 978-3-903176-37-9 © 2021 IFIP

$$\overset{(2)}{\Delta}_{\rm WP} - \overset{(2)}{\Delta}_{\rm PS} = \begin{cases} \dfrac{2\left[2B\rho^3 + \rho^2\left(5B+2\right) + \rho\left(4B+5\right) + B + 2\right]}{\mu^2\left[B\rho^3 + \rho^2\left(3B+1\right) + \rho\left(3B+2\right) + B + 1\right]}, & \text{if } \rho = \beta, \\ \dfrac{2\beta^{B+3}\left(1+\rho\right)^2\left(2\rho^3+\rho^2\right) - 2\rho^{B+3}\left[\left(\beta^3+\beta^2\right)\left(2\rho^2+3\rho\right) + \beta\left(\rho^2+\rho\right)\right]}{\mu^2\left(1+\rho\right)^2\left[\beta^{B+3}\rho^2\left(1+\rho\right) - \rho^{B+3}\beta^2\left(1+\beta\right)\right]}, & \text{otherwise,} \end{cases} \tag{26}$$

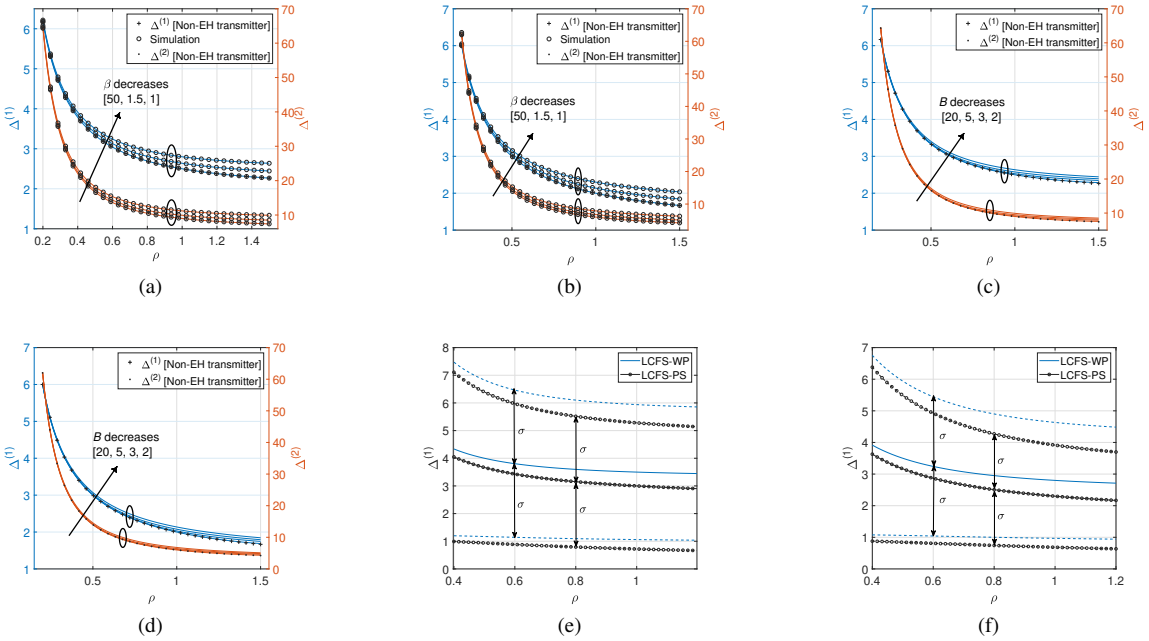

Fig. 3. Verification of the analytical results: (a) the LCFS-WP queueing discipline, and (b) the LCFS-PS queueing discipline. Impact of B on the achievable AoI performance: (c) the LCFS-WP queueing discipline, and (d) the LCFS-PS queueing discipline. Comparison between the LCFS-WP and LCFS-PS queueing disciplines: (e) $\beta = 0.5$, and (f) $\beta = 1$. We use $\mu = 1$ in all the figures, and $B = 2$ in (a), (b), (e) and (f).

achievable AoI by each queueing discipline. For instance, our results demonstrated that the second moment of AoI under the LCFS-WP queueing discipline is invariant to exchanging the arrival rates of status update and harvested energy packets. Our results also quantified the superiority of the LCFS-PS queueing discipline over the LCFS-WP one in terms of the achievable AoI performance. Several key system design insights were also drawn from our numerical results. For instance, our results quantified the improvement in the achievable AoI performance by each queueing discipline associated with the increase in either the battery capacity or the harvested energy arrival rate at the transmitter node. They also revealed that it is crucial to incorporate the higher moments of AoI in the design of real-time status update systems.

APPENDIX

A. Proof of Proposition 1

The steady state probabilities are the unique solution of the set of equations in (5), which can be expressed as

$$\eta\bar{\pi}_1 = \mu\bar{\pi}_3,\ (\eta+\lambda)\,\bar{\pi}_2 = \eta\bar{\pi}_1 + \mu\bar{\pi}_5,\ \mu\bar{\pi}_3 = \lambda\bar{\pi}_2, \tag{27}$$

$$(\eta+\lambda)\,\bar{\pi}_{2i} = \eta\bar{\pi}_{2i-2} + \mu\bar{\pi}_{2i+3}, 2 \le i \le B-1, \tag{28}$$

$$\mu\bar{\pi}_{2i+1} = \lambda\bar{\pi}_{2i}, 2 \le i \le B, \tag{29}$$

$$\sum_{i=1}^{2B+1} \bar{\pi}_i = 1. \tag{30}$$

From (27), we can express $\bar{\pi}_2$ and $\bar{\pi}_3$ as a function of $\bar{\pi}_1$ as $\bar{\pi}_2 = \frac{\beta}{\rho}\bar{\pi}_1$ and $\bar{\pi}_3 = \beta\bar{\pi}_1$. Next, using (28) and (29), $\bar{\pi}_{2i}$ and $\bar{\pi}_{2i+1}$, $1 \le i \le B$, can be expressed as in (12) and (13). Finally, by substituting (12) and (13) into (30), $\bar{\pi}_1$ can be expressed as $\bar{\pi}_1 = \frac{1}{1+\theta(1+\rho)}$, where $\theta = \sum_{i=1}^{B}\left(\frac{\beta}{\rho}\right)^i$. The final expression of $\bar{\pi}_1$ in (14) can be obtained by noting that $\theta = B$ if $\beta = \rho$, and $\theta = \frac{\left(\frac{\beta}{\rho}\right)^{B+1} - \frac{\beta}{\rho}}{\frac{\beta}{\rho}-1}$ otherwise. ■

B. Proof of Theorem 1

The set of equations in (8) can be expressed as

$$q_1: \ (\eta - s)\,[\bar{v}^s_{10}, \bar{v}^s_{11}] = \mu[\bar{v}^s_{31}, \bar{\pi}_3], \tag{31}$$

$$q_2: \ (\eta+\lambda-s)\,[\bar{v}^s_{20}, \bar{v}^s_{21}] = \mu[\bar{v}^s_{51}, \bar{\pi}_5] + \eta[\bar{v}^s_{10}, \bar{\pi}_1], \tag{32}$$

$$q_{2k}, 2 \le k \le B-1: \ (\eta+\lambda-s)\,[\bar{v}^s_{2k,0}, \bar{v}^s_{2k,1}] = \mu[\bar{v}^s_{2k+3,1}, \bar{\pi}_{2k+3}] + \eta[\bar{v}^s_{2k-2,0}, \bar{\pi}_{2k-2}], \tag{33}$$

$$q_{2B}: \ (\lambda - s)\,[\bar{v}^s_{2B,0}, \bar{v}^s_{2B,1}] = \eta[\bar{v}^s_{2B-2,0}, \bar{\pi}_{2B-2}]. \tag{34}$$

$$q_{2k+1}, 1 \le k \le B: \ (\mu - s)\,[\bar{v}^s_{2k+1,0}, \bar{v}^s_{2k+1,1}] = \lambda[\bar{v}^s_{2k,0}, \bar{\pi}_{2k}], \tag{35}$$

Summing the set of equations in (35) gives

$$(\mu - s)\sum_{k\in\,\mathrm{r}_2} \bar{v}^s_{k0} = \lambda\sum_{k\in\,\mathrm{r}_1} \bar{v}^s_{k0} - \lambda\bar{v}^s_{10}. \tag{36}$$

ISBN 978-3-903176-37-9 © 2021 IFIP

$$(\mu - s)\sum_{k\in\,\mathrm{r}_2}\bar{v}^s_{k1} = \lambda\sum_{k\in\,\mathrm{r}_1/\{1\}}\bar{\pi}_k. \tag{37}$$

Further, by summing (31)-(34), we have

$$(\lambda - s)\sum_{k\in\,\mathrm{r}_1}\bar{v}^s_{k0} = \mu\sum_{k\in\,\mathrm{r}_2}\bar{v}^s_{k1} + \lambda\bar{v}^s_{10}. \tag{38}$$

Now, from (8), the MGF of AoI at the destination can be evaluated as

$$\begin{aligned}\overset{\mathrm{WP}}{M}(\bar{s}) &= \sum_{k\in\,\mathrm{r}_1\cup\,\mathrm{r}_2}\bar{v}^s_{k0} \overset{(a)}{=} \frac{\lambda+\mu-s}{\mu-s}\sum_{k\in\,\mathrm{r}_1}\bar{v}^s_{k0} - \frac{\lambda}{\mu-s}\bar{v}^s_{10},\\ &\overset{(b)}{=} \frac{\rho\left(1+\rho-\bar{s}\right)}{\left(1-\bar{s}\right)^2\left(\rho-\bar{s}\right)}\sum_{k\in\,\mathrm{r}_1/\{1\}}\bar{\pi}_k + \frac{\rho}{\left(1-\bar{s}\right)\left(\rho-\bar{s}\right)}\bar{v}^s_{10},\\ &\overset{(c)}{=} \frac{\rho\left(1+\rho-\bar{s}\right)\bar{\pi}_1\theta}{\left(1-\bar{s}\right)^2\left(\rho-\bar{s}\right)} + \frac{\rho}{\left(1-\bar{s}\right)\left(\rho-\bar{s}\right)}\bar{v}^s_{10},\end{aligned} \tag{39}$$

where step (a) follows from substituting (36) into (39), step (b) follows from substituting (37) and (38) into (39), and step (c) follows from (12) in Proposition 1. Note that $\bar{v}^s_{10}$ can be obtained from (31) and (35) as $\frac{\beta\bar{\pi}_1}{(1-\bar{s})(\beta-\bar{s})}$. The final expression of $\overset{\mathrm{WP}}{M}(\bar{s})$ in (15) can be derived by substituting $\bar{v}^s_{10}$ into (39), followed by some algebraic simplifications. ∎

C. Proof of Theorem 2

We note from Fig. 2b that the set of equations in (8) corresponding to the states in r_1 are given by (31)-(34). Therefore, $\sum_{k\in\,\mathrm{r}_1}\bar{v}^s_{k0}$ can be expressed as in (38). On the other hand, for the states in r_2, we have

$$\begin{aligned}q_{2k+1}, 1\le k\le B:\ \ &(\lambda+\mu-s)\left[\bar{v}^s_{2k+1,0}, \bar{v}^s_{2k+1,1}\right] =\\ &\lambda[\bar{v}^s_{2k,0}, \bar{\pi}_{2k}] + \lambda[\bar{v}^s_{2k+1,0}, \bar{\pi}_{2k+1}].\end{aligned} \tag{40}$$

From (40), $\sum_{k\in\,\mathrm{r}_2}\bar{v}^s_{k0}$ is given by (36), and $\sum_{k\in\,\mathrm{r}_2}\bar{v}^s_{k1}$ can be expressed as

$$\sum_{k\in\,\mathrm{r}_2}\bar{v}^s_{k1} = \frac{\lambda\sum_{k\in\,\mathrm{r}_1\cup\,\mathrm{r}_2/\{1\}}\bar{\pi}_k}{\lambda+\mu-s} \overset{(a)}{=} \frac{\rho\left(1+\rho\right)\theta\bar{\pi}_1}{1+\rho-\bar{s}}, \tag{41}$$

where step (a) follows from Proposition 1. Hence, the MGF of AoI at the destination can be evaluated as

$$\begin{aligned}\overset{\mathrm{PS}}{M}(\bar{s}) &= \sum_{k\in\,\mathrm{r}_1\cup\,\mathrm{r}_2}\bar{v}^s_{k0} \overset{(a)}{=} \frac{\lambda+\mu-s}{\mu-s}\sum_{k\in\,\mathrm{r}_1}\bar{v}^s_{k0} - \frac{\lambda}{\mu-s}\bar{v}^s_{10}\\ &\overset{(b)}{=} \frac{\rho\left(1+\rho\right)\theta\bar{\pi}_1 + \rho\bar{v}^s_{10}}{\left(1-\bar{s}\right)\left(\rho-\bar{s}\right)}\\ &\overset{(c)}{=} \frac{\rho\left(1+\rho\right)\bar{\pi}_1\Big[\theta\left(\beta-\bar{s}\right)\left(1+\rho-\bar{s}\right)+\beta\Big]}{\left(1-\bar{s}\right)\left(\rho-\bar{s}\right)\left(1+\rho-\bar{s}\right)\left(\beta-\bar{s}\right)},\end{aligned} \tag{42}$$

where step (a) follows from substituting (36) into (42), and step (b) follows from substituting (38) and (41) into (42). Step (c) follows from substituting $\bar{v}^s_{10}$, obtained from (31), (40) and Proposition 1 as $\frac{\beta(1+\rho)\bar{\pi}_1}{(\beta-\bar{s})(1+\rho-\bar{s})}$. This completes the proof. ∎

REFERENCES

[1] M. A. Abd-Elmagid, N. Pappas, and H. S. Dhillon, "On the role of age of information in the Internet of things," *IEEE Commun. Magazine*, vol. 57, no. 12, pp. 72–77, Dec. 2019.

[2] S. Kaul, R. Yates, and M. Gruteser, "Real-time status: How often should one update?" in *Proc., IEEE INFOCOM*, 2012.

[3] S. K. Kaul, R. D. Yates, and M. Gruteser, "Status updates through queues," in *Proc., IEEE Conf. on Info. Sciences and Systems*, 2012.

[4] A. Soysal and S. Ulukus, "Age of information in G/G/1/1 systems: Age expressions, bounds, special cases, and optimization," 2019, available online: arxiv.org/abs/1905.13743.

[5] M. Costa, M. Codreanu, and A. Ephremides, "On the age of information in status update systems with packet management," *IEEE Trans. on Info. Theory*, vol. 62, no. 4, pp. 1897–1910, Apr. 2016.

[6] C. Kam, S. Kompella, G. D. Nguyen, J. E. Wieselthier, and A. Ephremides, "On the age of information with packet deadlines," *IEEE Trans. on Info. Theory*, vol. 64, no. 9, pp. 6419–6428, Sept. 2018.

[7] Y. Inoue, H. Masuyama, T. Takine, and T. Tanaka, "A general formula for the stationary distribution of the age of information and its application to single-server queues," *IEEE Trans. Info. Theory*, vol. 65, no. 12, pp. 8305–8324, Dec. 2019.

[8] J. P. Champati, H. Al-Zubaidy, and J. Gross, "On the distribution of AoI for the GI/GI/1/1 and GI/GI/1/2* systems: Exact expressions and bounds," in *Proc., IEEE INFOCOM*, 2019.

[9] F. Chiariotti, O. Vikhrova, B. Soret, and P. Popovski, "Peak age of information distribution for edge computing with wireless links," *IEEE Trans. on Commun.*, to appear.

[10] A. Kosta, N. Pappas, A. Ephremides, and V. Angelakis, "Non-linear age of information in a discrete time queue: Stationary distribution and average performance analysis," *IEEE Journal on Sel. Areas in Commun.*, to appear.

[11] R. D. Yates and S. K. Kaul, "The age of information: Real-time status updating by multiple sources," *IEEE Trans. on Info. Theory*, vol. 65, no. 3, pp. 1807–1827, Mar. 2019.

[12] R. D. Yates, "The age of information in networks: Moments, distributions, and sampling," *IEEE Trans. on Info. Theory*, vol. 66, no. 9, pp. 5712–5728, Sept. 2020.

[13] J. P. Hespanha, "Modelling and analysis of stochastic hybrid systems," *IEE Proceedings-Control Theory and Applications*, vol. 153, no. 5, pp. 520–535, Sept. 2006.

[14] S. K. Kaul and R. D. Yates, "Age of information: Updates with priority," in *Proc., IEEE Intl. Symposium on Information Theory*, 2018.

[15] R. D. Yates, "Status updates through networks of parallel servers," in *Proc., IEEE Intl. Symposium on Information Theory*, 2018.

[16] A. Javani, M. Zorgui, and Z. Wang, "Age of information in multiple sensing," in *Proc., Information Theory and its Applications (ITA)*, 2020.

[17] A. Maatouk, M. Assaad, and A. Ephremides, "On the age of information in a csma environment," *IEEE/ACM Trans. on Networking*, vol. 28, no. 2, pp. 818–831, Apr. 2020.

[18] M. Moltafet, M. Leinonen, and M. Codreanu, "Moment generating function of the AoI in a two-source system with packet management," *IEEE Wireless Commun. Letters*, to appear.

[19] R. D. Yates, "Lazy is timely: Status updates by an energy harvesting source," in *Proc., IEEE Intl. Symposium on Information Theory*, 2015.

[20] X. Zheng, S. Zhou, Z. Jiang, and Z. Niu, "Closed-form analysis of non-linear age of information in status updates with an energy harvesting transmitter," *IEEE Trans. on Wireless Commun.*, vol. 18, no. 8, pp. 4129–4142, Aug. 2019.

[21] S. Farazi, A. G. Klein, and D. R. Brown, "Average age of information for status update systems with an energy harvesting server," in *Proc., IEEE INFOCOM Workshops*, 2018.

[22] S. Farazi, A. G. Klein, and D. R. Brown, "Age of information in energy harvesting status update systems: When to preempt in service?" in *Proc., IEEE Intl. Symposium on Information Theory*, 2018.

[23] B. T. Bacinoglu, E. T. Ceran, and E. Uysal-Biyikoglu, "Age of information under energy replenishment constraints," in *Proc., Information Theory and its Applications (ITA)*, 2015.

[24] X. Wu, J. Yang, and J. Wu, "Optimal status update for age of information minimization with an energy harvesting source," *IEEE Trans. on Green Commun. and Networking*, vol. 2, no. 1, pp. 193–204, Mar. 2018.

[25] A. Arafa, J. Yang, S. Ulukus, and H. V. Poor, "Age-minimal transmission for energy harvesting sensors with finite batteries: Online policies," *IEEE Trans. on Info. Theory*, vol. 66, no. 1, pp. 534–556, Jan. 2020.

[26] M. A. Abd-Elmagid, H. S. Dhillon, and N. Pappas, "A reinforcement learning framework for optimizing age of information in RF-powered communication systems," *IEEE Trans. on Commun.*, vol. 68, no. 8, pp. 4747 – 4760, Aug. 2020.

[27] M. A. Abd-Elmagid, H. S. Dhillon, and N. Pappas, "AoI-optimal joint sampling and updating for wireless powered communication systems," *IEEE Trans. on Veh. Technology*, vol. 69, no. 11, pp. 14 110–14 115, Nov. 2020.

[28] M. A. Abd-Elmagid and H. S. Dhillon, "Closed-form characterization of the MGF of AoI in energy harvesting status update systems," 2021, available online: arxiv.org/abs/2105.07074.

ISBN 978-3-903176-37-9 © 2021 IFIP